

Published in final edited form as:

J Am Chem Soc. 2008 June 4; 130(22): 6942–6943.

Structure of a ^{129}Xe -Cryptophane Biosensor Complexed with Human Carbonic Anhydrase II

Julie A. Aaron, Jennifer M. Chambers, Kevin M. Jude, Luigi Di Costanzo, Ivan J. Dmochowski, and David W. Christianson

Roy and Diana Vagelos Laboratories, Department of Chemistry, University of Pennsylvania, Philadelphia, Pennsylvania 19104-6323

The α -carbonic anhydrases (CAs) are zinc metalloenzymes that catalyze the reversible hydration of CO_2 in forming HCO_3^- . The active site of an α -CA contains a catalytically essential Zn^{2+} coordinated by three histidine residues at the bottom of a 15 Å deep cleft, and the tightest binding CA inhibitors developed to date contain a sulfonamide moiety that coordinates to Zn^{2+} as a sulfonamidate anion.¹ Notably, human isozyme II (CAII) is an ideal model system for exploring new inhibitor designs, some of which can be exploited in biosensing applications.²⁻⁴ Here, CAII is utilized for the structure-based design of a xenon (^{129}Xe) biosensor for potential use as a magnetic resonance imaging (MRI) contrast agent.

The ^{129}Xe isotope has a spin-1/2 nucleus, a >200-ppm chemical shift window in water, and a natural isotopic abundance of 26% (commercially available up to 86%), which makes it an appealing biomolecular probe for MRI. Moreover, ^{129}Xe can be laser polarized to enhance MRI signals ~10,000-fold.⁵ Although current *in vivo* MRI applications are limited to functional lung imaging through the diffusion of Xe gas,⁶ the encapsulation of ^{129}Xe within a cryptophane cage ($K_D \approx 30 \mu\text{M}$ at 37 °C in phosphate-buffered solution)⁷ facilitates its use as a biosensor that can be targeted to specific proteins using an appropriate affinity tag.^{8,9} For example, racemic biosensor **1** (Figure 1a) has been designed to bind to the CA isozymes ($K_D = 60 \pm 20 \text{ nM}$ against CAII in solution), and yields a distinctive ^{129}Xe -MRI spectrum when bound to CAII.¹⁰ Here, we report the X-ray crystal structure of the CAII-**1**-Xe complex at 1.70 Å resolution.

For structure determination, CAII was overexpressed in *E. coli* and purified as described,¹¹ then incubated with a two-fold excess of **1**, concentrated to 10 mg/mL, and crystallized by the hanging drop vapor diffusion method. Crystals were cryoprotected in 15% glycerol and subsequently pressurized under 20 atm Xe for 30 min prior to flash cooling and X-ray data collection. The structure was refined to final R_{work} and R_{free} values of 0.23 and 0.25, respectively.

Biosensor **1** coordinates to the active site Zn^{2+} ion as the sulfonamidate anion, displacing the zinc-bound hydroxide ion of the native enzyme as previously observed in other complexes of CAII with benzenesulfonamide derivatives.^{1,2,12} The crystallographic occupancies of **1** and Zn^{2+} are refined at 0.5. It is unusual to observe diminished Zn^{2+} occupancy in a CAII-inhibitor complex, but the molecular origins of this effect are not clear.

The encapsulation of Xe within the cryptophane cage of **1** is confirmed by inspection of the Bijvoet difference Fourier map calculated from anomalous scattering data (Figures 1b and S1.) X-ray diffraction data was collected at a wavelength $\lambda = 0.9795 \text{ \AA}$, which is far from the Xe L_I edge of 2.27 Å.¹³ Nevertheless, the anomalous scattering component f' is 3.4 e^- for Xe, so

the anomalous signal is still prominent at the wavelength of data collection. A second Xe binding site is observed in a hydrophobic pocket defined by A116, L148, V218, L157, V223 and F226 (Figure S2). The crystallographic occupancies of these Xe sites refine to 0.50 and 0.37, respectively. Anomalous scattering peaks are absent from crystals not subject to Xe pressurization.

Notably, **1** contains a chiral axis and the electron density map reveals the binding of equal populations of both enantiomers, (each refined with an occupancy of 0.25; Figure 1)¹⁴⁻¹⁶ Overall, the binding of **1** does not cause any significant structural changes in the active site, and the root-mean-square deviation is 0.34 Å for 256 C α atoms between the current structure and the unliganded enzyme (PDB 2CBA).¹⁷

The total surface area of **1** is ~1500 Å², of which ~500 Å² becomes solvent inaccessible due to contacts of **1** within the active site cleft of CAII designated molecule I in Figure 2. The surrounding CAII molecules in the unit cell (molecules II-IV), sequester an additional ~540 Å² of the surface area of **1** from solvent. Some structural changes are observed near the outer rim of the active site cleft where the cryptophane binds. The most notable change is observed for Q136, which rotates ~180° to make van der Waals contacts with the cryptophane and the symmetry-related cryptophane bound to molecule III in the crystal lattice. Other residues at the active site rim of molecule I that make close contacts with the cryptophane are G132 and P202. Additional structural changes in the crystal lattice result from the binding of **1** to molecule I: in molecule II, H36 rotates ~90° to make a van der Waals contact with the cage, and Q137 of molecule III rotates ~90° to donate a hydrogen bond to an ether oxygen atom of **1**.

Although the pendant propionates appear to be more disordered than the cryptophane and are characterized by correspondingly weaker electron density, a hydrogen bond between a propionate moiety and Q53 of molecule II is observed. The relative dearth of strong cryptophane-protein interactions may explain why the affinity of **1** measured by ITC is only slightly better than that measured for the parent triazole-benzenesulfonamide lacking the cryptophane ($K_D = 100 \pm 10$ nM).¹⁰

Limited hydrogen bond interactions between CAII and the cryptophane moiety of **1** may be advantageous for the use of cryptophanes as ¹²⁹Xe biosensors. Translational and rotational freedom, the consequence of a flexible linker between the cryptophane and the benzenesulfonamide, could allow the cage to reorient rapidly *in situ*, independently of the protein, to result in decreased correlation times and narrower line widths that increase the sensitivity of ¹²⁹Xe NMR measurements in solution.⁸

In conclusion, this work reveals the first experimentally determined structure showing how an encapsulated ¹²⁹Xe atom can be specifically directed to a biomedically relevant protein target. The possible implications for cancer diagnosis are profound, given that CA isozymes IX and XII are overexpressed on the surface of certain cancer cells.¹⁸ Moreover, a search of the Protein Data Bank reveals that with its molecular mass of 1554, the **1**-Xe complex is one of the largest synthetic organic ligands ever cocrystallized with a protein. Thus, this work demonstrates the feasibility of preparing crystalline complexes between proteins and nonbiological, nanometer-scale ligands.¹⁹

Supplementary Material

Refer to Web version on PubMed Central for supplementary material.

Acknowledgement

We thank the Advanced Light Source and the Cornell High Energy Synchrotron Source beamline F-2 for access to X-ray crystallographic data collection facilities and Ulrich English for support with the Xe chamber experiments. We

also thank P.A. Hill for helpful discussions. I.J.D. is a Camille and Henry Dreyfus Teacher-Scholar and thanks DOD for grant W81XWH-04-1-0657. Finally, we thank the NIH for a Chemical Biology Interface training grant (to J.A.A.), 1R21CA110104 (to I.J.D.) and GM49758 (to D.W.C.). D.W.C. also thanks the BBSRC for the Underwood Fellowship.

References

- (1). Supuran CT, Scozzafava A. *Bioorg. Med. Chem* 2007;15:4336–4350. [PubMed: 17475500]
- (2). Elbaum D, Nair SK, Patchan MW, Thompson RB, Christianson DWJ. *Am. Chem. Soc.* 1996;118:8381–8387.
- (3). Krishnamurthy VM, Kaufman GK, Urbach AR, Gitlin I, Gudiksen KL, Weibel DB, Whitesides GM. *Chem. Rev* 2008;108:946–1051. [PubMed: 18335973]
- (4). Bozym RA, Thompson RB, Stoddard AK, Fierke CA. *ACS Chem. Biol* 2006;1:103–111. [PubMed: 17163650]
- (5). Cherubini A, Bifone A. *Prog. Nucl. Magn. Reson. Spectrosc* 2003;42:1–30.
- (6). Fain SB, Korosec FR, Holmes JH, O'Halloran R, Sorkness RL, Grist TM. *J. Magn. Reson. Imaging* 2007;25:910–923. [PubMed: 17410561]
- (7). Hill PA, Wei Q, Eckenhoff RG, Dmochowski IJ. *J. Am. Chem. Soc* 2007;129:9262–9263. [PubMed: 17616197]
- (8). Lowery TJ, Garcia S, Chavez L, Ruiz EJ, Wu T, Brotin T, Dutasta JP, King DS, Schultz PG, Pines A, Wemmer DE. *ChemBioChem* 2006;7:65–73. [PubMed: 16342304]
- (9). Schröder L, Lowery TJ, Hilty C, Wemmer DE, Pines A. *Science* 2006;314:446–449. [PubMed: 17053143]
- (10). Chambers, JM.; Hill, PA.; Aaron, JA.; Han, Z.; Christianson, DW.; Kuzma, NN.; Dmochowski, IJ. Manuscript in preparation
- (11). Alexander RS, Kiefer LL, Fierke CA, Christianson DW. *Biochemistry* 1993;32:1510–1518. [PubMed: 8431430]
- (12). Eriksson AE, Kylsten PM, Jones TA, Liljas A. *Proteins: Struct. Funct. Gen* 1988;4:283–293.
- (13). Watanabe T. *Phys. Rev* 1965;137:1380–1382.
- (14). Collet, A. *Comprehensive Supramolecular Chemistry*. Atwood, JL.; Davis, JED.; MacNicol, DD.; Vogtle, F., editors. 2. Pergamon; New York: 1996. p. 325-365. Chapter 11
- (15). Ruiz EJ, Sears DN, Pines A, Jameson CJ. *J. Am. Chem Soc* 2006;128:16980–16988. [PubMed: 17177449]
- (16). Eliel, EL.; Wilen, SH. *Stereochemistry of Organic Compounds*. John Wiley & Sons, Inc.; New York: 1994. p. 1119-1190.
- (17). Håkansson K, Carlsson M, Svensson LA, Liljas A. *J. Mol. Biol* 1992;227:1192–1204. [PubMed: 1433293]
- (18). Pastorekova S, Parkkila S, Zavada J. *Adv. Clin. Chem* 2006;42:167–216. [PubMed: 17131627]
- (19). The atomic coordinates of the human carbonic anhydrase II-sulfonamide cryptophane-A complex have been deposited in the Protein Data Bank with accession code 3CYU

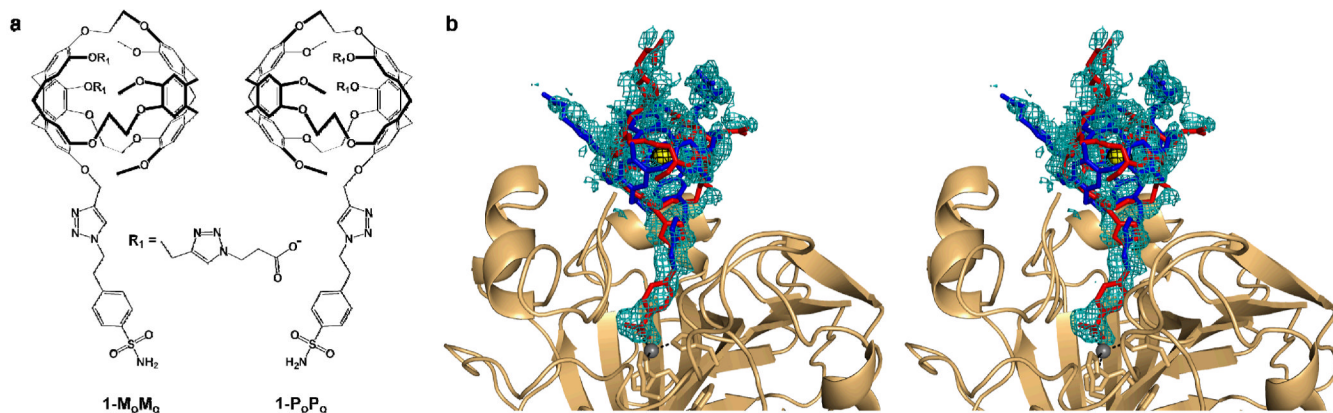


Figure 1.

(a) The M_0M_0 and P_0P_0 enantiomers of the cryptophane-A-derived CA biosensor. The benzenesulfonamide moiety serves as an affinity tag that targets the Zn^{2+} ion, and the R_1 substituents contain triazole propionate moieties that enhance aqueous solubility. (b) Stereoview of a simulated annealing omit map showing $1-M_0M_0$ (blue) and $1-P_0P_0$ (red) bound in the active site (1.9σ contour, teal). A Bijvoet difference Fourier map (2.0σ , black) confirms the encapsulation of Xe (yellow). Coordination interactions with Zn^{2+} (grey sphere) are indicated by dotted lines.

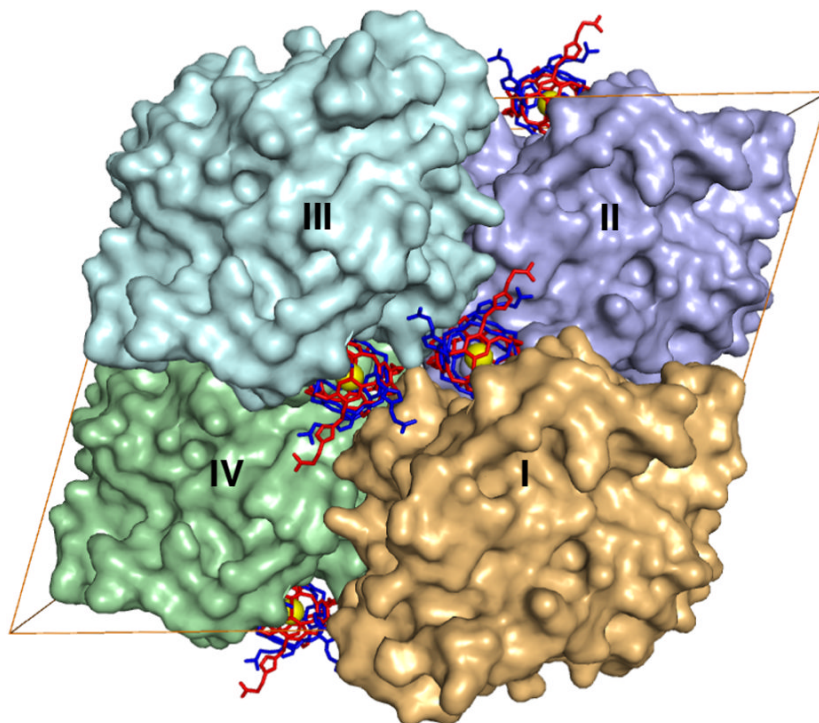


Figure 2. The unit cell of CAII crystals in space group $C2$ contains four molecules: I (x,y,z), II ($x+1/2,y+1/2,z$), III ($-x,y,-z$) and IV ($-x+1/2,y+1/2,-z$). The binding of **1** in the active site cleft of molecule I buries $\sim 500 \text{ \AA}^2$. Crystal contacts bury an additional 540 \AA^2 of the surface of **1** as follows: 270 \AA^2 with molecule III, and 240 \AA^2 and 30 \AA^2 with the front and back faces of molecule II, respectively. Molecule IV does not contact **1** bound to molecule I.